Article

Thermodynamic analysis and systematic comparison of solar-heated trigeneration systems based on ORC and absorption heat-pump

Jesús García-Domínguez [1]* and J. Daniel Marcos [1]

[1] Universidad Nacional de Educación a Distancia, UNED, Madrid, Spain;
* Correspondence: jesus.gdominguez@gmail.com

Abstract: Modular and scalable distributed generation solutions as combined cooling, heating and power (CCHP) systems are currently a promising solution for the simultaneous generation of electricity and useful heating and cooling for large buildings or industries. In the present work, a solar-heated trigeneration approach based on different Organic Rankine Cycle (ORC) layouts and a single-effect H_2O/LiBr absorption heat-pump integrated as a bottoming cycle is analysed from the thermodynamic viewpoint. The main objective of the study is to provide a comprehensive guide for selecting the most suitable CCHP configuration for a solar-heated CCHP system following a systematic investigation approach. Six alternative CCHP configurations based on single-pressure and dual-pressure ORC layouts, such as simple, recuperated, and superheated cycles, and their combinations, and seven organic fluids as working medium are proposed and compared systematically. A field of Solar Parabolic Trough Collectors (SPTCs) used as a heat source of the ORC layouts and the absorption heat-pump are kept invariant. A comprehensive parametric analysis of the different proposed configurations is carried out for different design parameters. Several output parameters, such as energy and exergy efficiency, net electrical power, and electrical to heating and cooling ratios are examined. The study reveals that the most efficient CCHP configuration is the single-pressure ORC recuperated and superheated cycle with toluene as a working fluid, which is on average 25% and 8% more efficient than the variants with single-pressure simple cycle and the dual-pressure recuperated superheated cycle, respectively. At nominal design conditions, the best performing CCHP variant presents 163.7% energy efficiency, 12.3% exergy efficiency, while the electricity, cooling and heating productions are 56.2 kW, 223.0 kW and 530.1 kW respectively.

Keywords: Trigeneration (CCHP); Organic Rankine Cycle (ORC); Solar thermal energy; Parametric optimization; Performance comparison

1. Introduction

One of the potential applications that combine the use of low or medium temperature solar energy and Organic Rankine Cycle (ORC) is a trigeneration thermal system, which can be defined as combined cooling, heating, and power (CCHP) production simultaneously from the same energy source [1]. In this regard, the thermodynamic analysis to optimise the performance of this system is an important area of research to improve energy efficiency.

In particular for ORC technology, in the last few years different investigations have been carried out aimed at evaluating its technical, economic and market penetration differentiating its wide range of application according to the driven energy source [2-7]. In order to compare different configurations of the ORC system and different working fluids, Branchini et al. [8] carried out a parametric analysis through different performance indexes, concluding that both the evaporation pressure and the maximum temperature of the heat source are determining parameters in the performance of the power cycle.

Delgado-Torres et al. [9] carried out an analysis and optimization of a low temperature solar driven ORC system considering different solar collector technologies as well as different cycle configurations and organic working fluids. The results obtained indicate that a recovery stage downstream of the turbine implies higher average temperatures in the cycle, and therefore, higher cycle efficiency.

Likewise, for CCHP systems based on ORC power cycle, several studies were done in recent years to determine the thermal and economic performance for different system configurations [10-15]. Al-Sulaiman et al. [16] analysed and compared three CCHP systems with different prime mover approaches: a solid oxide fuel cell (SOFC), a biomass boiler, and SPTCs. The results indicated that the maximum electrical efficiency is achieved for the SOFC system with a value of 19%, being 15% for the biomass system; and 15% for the solar energy system. Al-Sulaiman et al. [17] designed and assessed a trigeneration system driven by Solar Parabolic Trough Collectors (SPTCs) to produce 500 kW of electricity through an ORC system. The results show that the maximum electrical efficiency is 15%, while the overall efficiency of the CCHP is 94%. Suleman et al. [18] proposed a new system combining solar and geothermal energy as prime movers for multigeneration applications. The overall energy and exergy efficiencies of the system are found to be 54.7% and 76.4%, respectively. Bellos and Tzivanidis [19] analysed a solar-driven CCHP system through a parametric optimization for different working fluids and design parameters. In the optimum case, the electric exergy and energy efficiency found are 27.9% and 22.5%, respectively, while the energetic performance varied from 130% to 180%.

The use of SPTCs in combination with different ORC layouts and absorption heat-pumps for trigeneration systems have been already examined to date. However, there are no known studies aimed at optimizing solar-powered trigeneration systems by means of systematic comparison of multiple ORC configuration and the correspondent parametric analysis. Therefore, the current investigation has a significant contribution by analyzing and optimizing the use of concentrated solar energy and ORC technology as a prime mover for a trigeneration plant. In this paper the performance of six alternative CCHP configurations based on single-pressure and dual-pressure ORC layouts, such as simple, recuperated, and superheated cycles, and their combinations, is analysed and compared considering seven working fluids. All the analysed CCHP configurations are fed with thermal input from SPTCs through a close loop that constrains the minimum temperature of the heat source at the evaporator outlet. A single-effect H_2O/LiBr absorption heat-pump is integrated as a bottoming cycle to meet heating and cooling demands simultaneously.

The objective of this work is twofold: on one hand, to provide a comprehensive guide for selecting the most suitable solar-heated CCHP configuration in terms of system energy and exergy efficiency by means of a fair systematic comparison between the six layouts and the seven working fluids, on the other, to evaluate parametrically all the CCHP alternatives for a wide range of solar field outlet temperature and ORC condensation temperature enabling the design of the most efficient system that may be coupled with buildings or industries for combined generation, or as a back-up, of electricity, cooling and heating.

2. Thermodynamic analysis of CCHP solutions

The CCHP system assessed in this study is mainly composed of an ORC as a power generator which is driven by a field of SPTCs. Six alternative ORC layouts are compared under steady-state conditions and seven organic fluids are considered as working medium are proposed. A single-effect H_2O/LiBr absorption heat-pump is integrated as a bottoming cycle to meet heating and cooling demands simultaneously.

2.1. Investigated thermodynamic CCHP configurations

In order to determine the most suitable solar-heated CCHP configuration, a thermodynamic analysis is conducted for the six configurations represented in Figures 1-6. The six power cycles are: (i) single-pressure simple cycle (1P SC), (ii) single-pressure superheated cycle (1P SH), (iii) single-pressure recuperated cycle (1P REC), (iv) single-pressure recuperated superheated cycle (1P REC+SH), (v) single-pressure regenerative recuperated superheated cycle (1P REG+REC+SH), and (vi) dual-pressure recuperated superheated cycle (2P REC+SH).

The selection of the appropriate working fluid plays a very important role in the system design as the ORC energy and exergy efficiency must be as high as possible, and the fluid must be chemically stable in the selected working temperature range. Environmental and safety issues must also be considered. For the present work, seven organic working fluids have been selected in order to deal with solar field outlet temperature values between 180 ºC and 260 ºC, typical values for a field of SPTCs used in existing ORC systems.

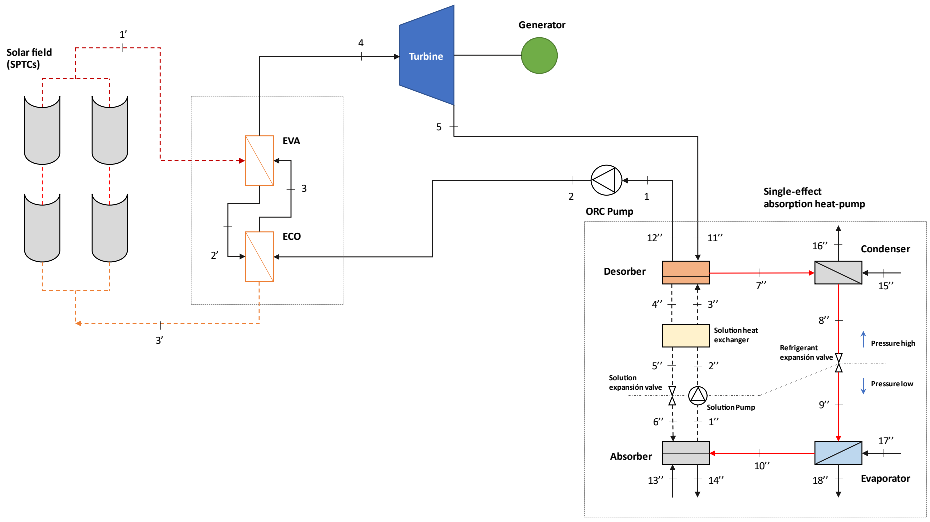

Figure 1. Case 1: CCHP with single-pressure ORC Simple cycle (1P SC)

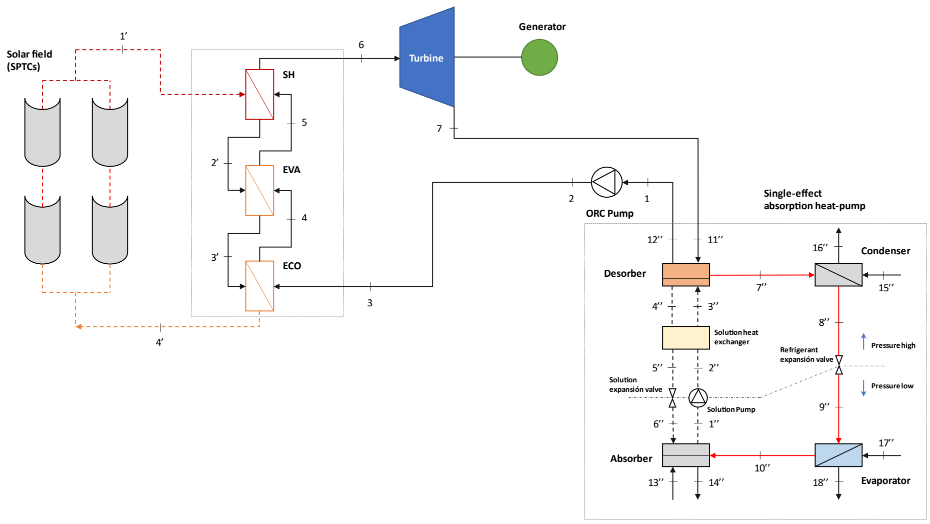

Figure 2. Case 2: CCHP with single-pressure ORC superheated cycle (1P SH)

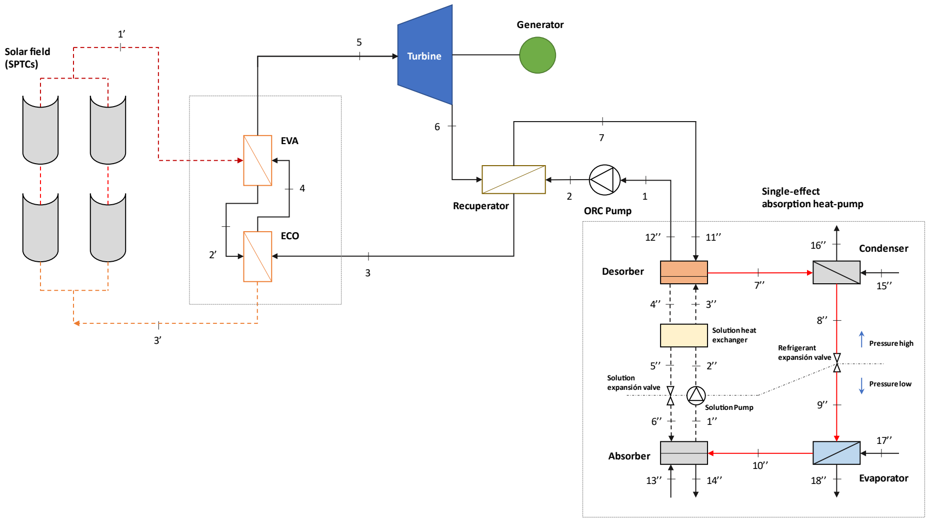

Figure 3. Case 3: CCHP with single-pressure ORC recuperated cycle (1P REC)

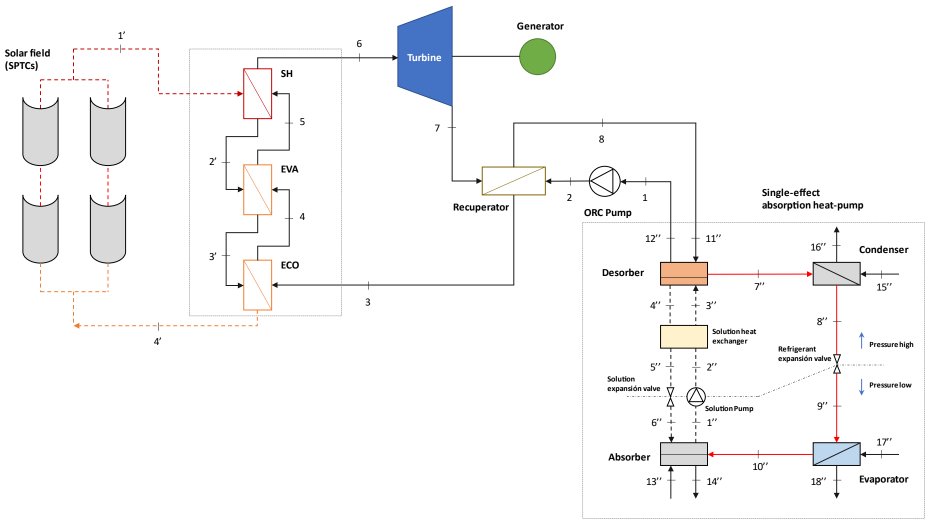

Figure 4. Case 4: CCHP with single-pressure ORC recuperated superheated cycle (1P REC+SH)

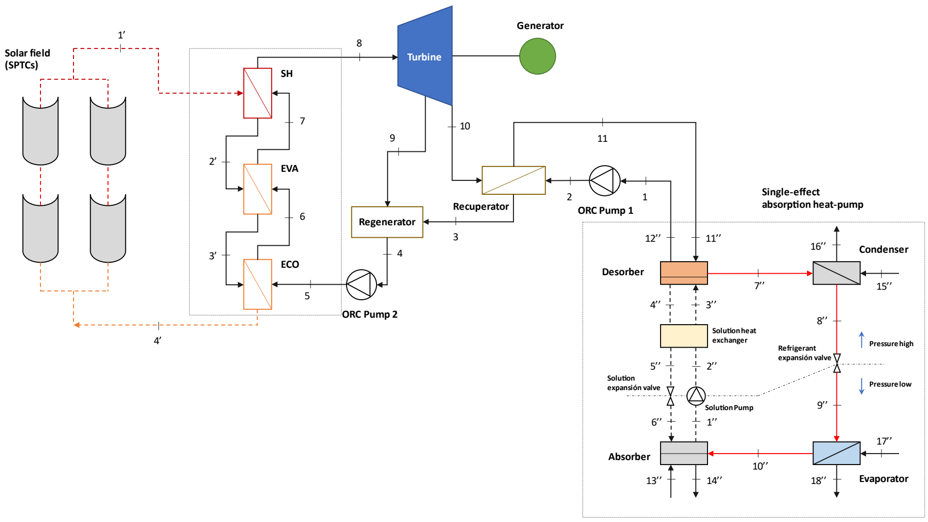

Figure 5. Case 5: CCHP with single-pressure ORC regenerative recuperated superheated cycle (1P REG+REC+SH)

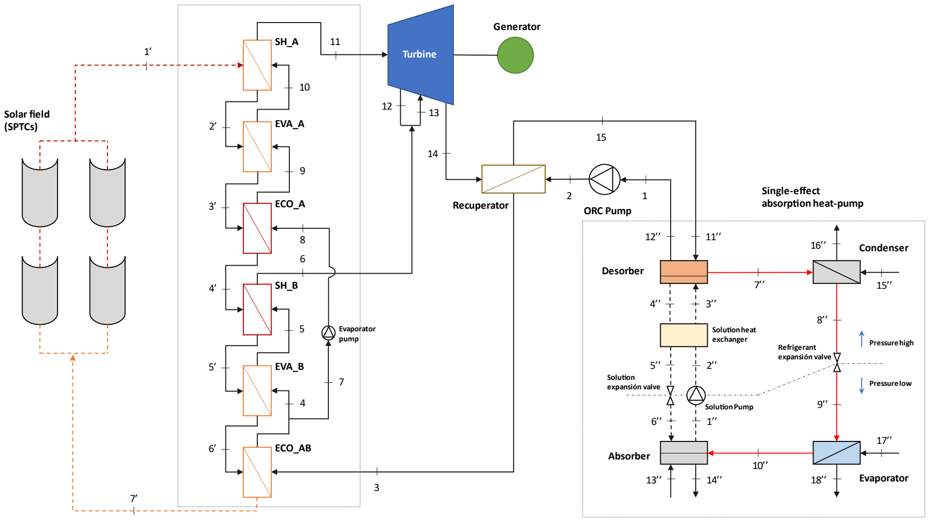

Figure 6. Case 6: CCHP with dual-pressure ORC recuperated superheated cycle (2P REC+SH).

2.2. CCHP performance indexes

The overall performance assessment equations of the CCHP considered are presented in this section. The energy and exergy efficiency of the ORC are calculated taking into account the efficiency of SPTC. The Petela model is used for the exergy flow of the solar irradiation [20].

$$
\begin{aligned}
\eta_{en,ORC} &= \frac{W_{turb}-W_{ORC,pump}}{Q_{sol}}\;; && \textit{for Case 1-4}\\
\eta_{en,ORC} &= \frac{W_{turb}-W_{ORC,pump1}-W_{ORC,pump2}}{Q_{sol}}\;; && \textit{for Case 5}\\
\eta_{en,ORC} &= \frac{W_{turb}-W_{ORC,pump1}-W_{Evap,pump}}{Q_{sol}}\;; && \textit{for Case 6}
\end{aligned}
\tag{1}
$$

$$
\begin{aligned}
\eta_{ex,ORC} &= \frac{W_{turb}-W_{ORC,pump}}{Q_{sol}\cdot\left(1-\frac{4}{3}\cdot\frac{T_0}{T_{sun}}+\frac{1}{3}\cdot\left(\frac{T_0}{T_{sun}}\right)^4\right)}\;; && \textit{for Case 1-4}\\
\eta_{ex,ORC} &= \frac{W_{turb}-W_{ORC,pump1}-W_{ORC,pump2}}{Q_{sol}\cdot\left(1-\frac{4}{3}\cdot\frac{T_0}{T_{sun}}+\frac{1}{3}\cdot\left(\frac{T_0}{T_{sun}}\right)^4\right)}\;; && \textit{for Case 5}\\
\eta_{ex,ORC} &= \frac{W_{turb}-W_{ORC,pump1}-W_{Evap,pump}}{Q_{sol}\cdot\left(1-\frac{4}{3}\cdot\frac{T_0}{T_{sun}}+\frac{1}{3}\cdot\left(\frac{T_0}{T_{sun}}\right)^4\right)}\;; && \textit{for Case 6}
\end{aligned}
\tag{2}
$$

where:

$$
\begin{aligned}
W_{turb} &= \dot{m}_{ORC}\cdot(h_4-h_5)\;; && \textit{for Case 1}\\
W_{turb} &= \dot{m}_{ORC}\cdot(h_6-h_7)\;; && \textit{for Case 2, 4}\\
W_{turb} &= \dot{m}_{ORC}\cdot(h_5-h_6)\;; && \textit{for Case 3}\\
W_{turb} &= (\dot{m}_{ORC,A}+\dot{m}_{ORC,B})\cdot h_8-\dot{m}_{ORC,A}\cdot h_9-\dot{m}_{ORC,B}\cdot h_{10}\;; && \textit{for Case 5}\\
W_{turb} &= \dot{m}_{ORC,A}\cdot(h_{11}-h_{12})+(\dot{m}_{ORC,A}+\dot{m}_{ORC,B})\cdot(h_{13}-h_{14})\;; && \textit{for Case 6}
\end{aligned}
\tag{3}
$$

$$
\begin{aligned}
W_{ORC,pump} &= \dot{m}_{ORC}\cdot(h_2-h_1)\;; && \textit{for Case 1-4}\\
W_{ORC,pump1} &= \dot{m}_{ORC}\cdot(h_2-h_1)\;; && \textit{for Case 5}
\end{aligned}
\tag{4}
$$

$$W_{ORC,pump2} = \dot{m}_{ORC} \cdot (h_5 - h_4) \;; \qquad \textit{for Case 5}$$
$$W_{Evap,pump} = \dot{m}_{ORC} \cdot (h_8 - h_7) \;; \qquad \textit{for Case 6}$$
$$Q_{sol} = DNI \cdot w_{ap} \cdot L_{SPTC} \cdot N_{SPTC} \tag{5}$$

The efficiency of the cooling-cogeneration and the efficiency of the trigeneration are defined as

$$\eta_{en,tri} = \left(\frac{W_{turb} - W_{ORC,pump} + Q_e + Q_a + Q_c}{Q_{sol}}\right) \;; \qquad \textit{for Case 1-4}$$
$$\eta_{en,tri} = \left(\frac{W_{turb} - W_{ORC,pump1} - W_{ORC,pump2} + Q_e + Q_a + Q_c}{Q_{sol}}\right) \;; \qquad \textit{for Case 5} \tag{6}$$
$$\eta_{en,tri} = \left(\frac{W_{turb} - W_{ORC,pump} - W_{Evap,pump} + Q_e + Q_a + Q_c}{Q_{sol}}\right) \;; \qquad \textit{for Case 6}$$

$$\eta_{ex,\mathrm{tri}} = \left(\frac{W_{turb} - W_{ORC,pump} + Q_e \cdot (t_0/t_{17}'' - 1) + (Q_a + Q_c) \cdot (1 - t_0/t_{13}'')}{Q_{sol} \cdot \left(1 - \frac{4}{3} \cdot \frac{T_0}{T_{sun}} + \frac{1}{3} \cdot \left(\frac{T_0}{T_{sun}}\right)^4\right)}\right) \;; \qquad \textit{for Case 1-4}$$
$$\eta_{ex,\mathrm{tri}} = \left(\frac{W_{turb} - W_{ORC,pump1} - W_{ORC,pump2} + Q_e \cdot (t_0/t_{17}'' - 1) + (Q_a + Q_c) \cdot (1 - t_0/t_{13}'')}{Q_{sol} \cdot \left(1 - \frac{4}{3} \cdot \frac{T_0}{T_{sun}} + \frac{1}{3} \cdot \left(\frac{T_0}{T_{sun}}\right)^4\right)}\right) \;; \qquad \textit{for Case 5} \tag{7}$$
$$\eta_{ex,\mathrm{tri}} = \left(\frac{W_{turb} - W_{ORC,pump} - W_{Evap,pump} + Q_e \cdot (t_0/t_{17}'' - 1) + (Q_a + Q_c) \cdot (1 - t_0/t_{13}'')}{Q_{sol} \cdot \left(1 - \frac{4}{3} \cdot \frac{T_0}{T_{sun}} + \frac{1}{3} \cdot \left(\frac{T_0}{T_{sun}}\right)^4\right)}\right) \;; \qquad \textit{for Case 6}$$

The coefficient of performance (COP) of the heat-pump for cooling and heating mode is defined as

$$COP_{cool} = \frac{Q_e}{Q_d + W_{S.pump}} \quad (8) \qquad ; \qquad COP_{heat} = \frac{Q_c + Q_a}{Q_d + W_{S.pump}} \quad (9)$$

2.3. CCHP thermodynamic calculation procedure and numerical assumptions

The mathematical modelling of the proposed trigeneration system with all its variants is based on mass and energy balances applied to each component of the system under steady-state conditions. For a given configuration and a given working fluid, the inlet and outlet thermodynamic states of each component are calculated on the basis of the same given input data and assumptions using Engineering Equations Solver (EES) software.

The energy formulations of the SPTC are based on the equations presented in [16] for an absorber pipe with glass envelope as shown in Figure 7. The energy balance in a section of the absorber pipe depends mainly on: *i)* Radiation losses from the glass envelope to the open sky ($\dot{q}'_{57rad}$); *ii)* Convection losses from the glass envelope to the environment ($\dot{q}'_{56conv}$); *iii)* Radiation losses from the selective coating of the metal tube to the glass envelope ($\dot{q}'_{34rad}$); *iv)* Conduction losses through metal pipe supports ($\dot{q}'_{cond,bracket}$).

All heat losses described in this section are evaluated in an analytical manner using the thermodynamic and fluid-mechanical equations and correlations governing heat transfers by conduction, convection and radiation. A stationary energy balance for the cross-section of the absorber pipe is then propose applying the principle of energy conservation to each of the surfaces of the section. Due to the complexity involved in this type of development, numerous simplifying hypotheses have been made. Most of these assumptions are made considering that temperatures, heat fluxes and thermodynamic properties are uniform around the perimeter of the absorber pipe.

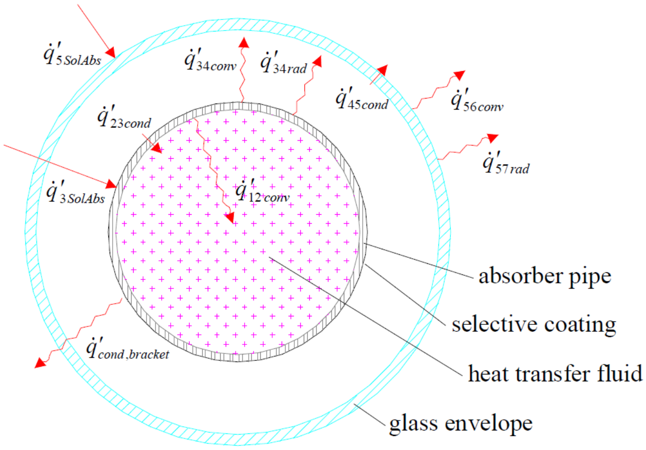

Figure 7. This is a figure. Schemes follow the same formatting.

Absorber inner surface. The useful heat that the solar thermal oil receives is the result of transfer by conduction through the absorber tube.

$$\dot{q}'_{12conv} = \dot{q}'_{23cond} \tag{10}$$

Absorber outer surface. The heat that the surface of the absorber receives from the sun, after taking into account both the optical and geometric effects of the collector, is the result of the sum of the heat fluxes due to the absorber-glass radiation, internal convection, heat loss through the absorber pipe support brackets and the fraction of energy that is finally conducted through the thickness of the absorber pipe into the fluid.

$$\dot{q}'_{3SolAbs} = \dot{q}'_{23cond} + \dot{q}'_{34rad} + \dot{q}'_{34conv} + \dot{q}'_{cond,bracket} \tag{11}$$

Glass envelope inner surface. The heat that is evacuated from the absorber outer surface through the space between the absorber and the glass envelope (regardless of whether there is a vacuum or not) is the same as that is transferred by conduction through the thickness of the glass.

$$\dot{q}'_{34rad} + \dot{q}'_{34conv} = \dot{q}'_{45cond} \tag{12}$$

Glass envelope outer surface. The heat that falls upon the external surface is in balance with the heat that the system releases to the outside from the external surface of the glass envelope.

$$\dot{q}'_{5SolAbs} + \dot{q}'_{45cond} = \dot{q}'_{56conv} + \dot{q}'_{57rad} \tag{13}$$

Considering that the region between the absorber pipe and the glass envelope has been vacuumed, the convective heat transfer between the two surfaces ($\dot{q}'_{34conv}$) can be considered negligible. Hence, under these assumptions, the useful thermal power ($\dot{q}'_{12conv}$) can be reformulated as follows:

$$\dot{q}'_{util} = \dot{q}'_{3SolAbs} + \dot{q}'_{5SolAbs} - (\dot{q}'_{56conv} + \dot{q}'_{57rad} + \dot{q}'_{cond,bracket}) \tag{14}$$

The overall efficiency of the SPTC considers all types of losses: optical, geometric and thermal, and can be defined as the ratio between the useful thermal power delivered to the solar thermal oil, and the solar resource available based on the Direct Normal Irradiance (*DNI*).

$$\eta_{SPTC} = \frac{\dot{q}'_u}{\dot{q}'_{sol}} = \frac{\dot{q}'_u}{DNI \cdot w_{ap}} \tag{15}$$

where $\dot{q}'_u$ is defined as

$$\dot{q}'_u = \frac{\dot{m}_{sol} Cp_{sol}(T_{sol.out} - T_{sol.in})}{L_{SPTC}} \tag{16}$$

The solar field includes SPTCs (PTMx-24 from the company Soltigua) with a total collecting area of 617,4 m^2, consisting of five rows with two collectors per row. The specifications of the collector and the parameters of the solar system that have been selected in this analysis are defined in Table 1. The selected values are reasonable, and they were taken from Refs [9, 17, 19, 21].

Table 1. Input data for SPTC model

Parameter	Value
Collector aperture width, – w_{ap}	2.36 m
Collector length – L_{SPTC}	26.16 m
Collector nominal mass flow rate	1 kg/s
Absorber outer diameter	20.5 mm
Absorber inner diameter	22 mm
Glass envelope outer diameter	37.5 mm
Glass envelope inner diameter	40 mm
Number of collectors - N_{SPTC}	10
Solar field outlet temperature – $T_{1'}$	200 ºC
Ambient temperature	30 ºC
Reference temperature	298.15 K
Sun Temperature	5,770 K
Direct Normal Irradiance – *DNI*	800 W/m^2
Solar incident angle	0 º
Wind velocity	3 m/s

The ORC modelling is performed for the six CCHP configuration variants represented in Figure 1-6. Apart of the inputs coming from solar field model, which are the solar field outlet temperature and mass flow rate, the key input thermodynamic variables required for the calculations are:

- The turbine isentropic efficiency;
- The ORC pump isentropic efficiency;
- For SH cycles, the superheating temperature;
- For REC cycles, the recuperator effectiveness;
- The condensation temperature;

The evaporator, so called heat recovery system, is the element that serves as the link between the heat source, provided by the SPTCs, and the steam cycle. In the evaporator the fluid passes through different stages depending on the ORC layout considered. Initially in the economizer the fluid is heated to the fluid evaporation temperature minus a Delta T, so called Approach Point (AP); in the evaporator, heat is added to the saturated liquid to produce saturated vapor at constant temperature and pressure. In case a superheater is considered, the saturated vapor is heated above the evaporation temperature until design conditions. The evaporator design parameters used in the study are the Pinch Point (PP) - *difference between the solar field mass flow and the organic fluid* -, the Approach Point (AP) - *difference between the organic fluid temperature leaving the evaporator and the saturation temperature* -, and the live steam outlet temperature T_{LS}. All these values are given in Table 2. The Figure 8 represents the schemes and heat transfer-temperature diagrams for a single-pressure evaporator with superheater, that applies to Case 2, 4- 5, and for a dual-pressure evaporator with low-pressure and high-pressure superheaters, that applies to Case 6.

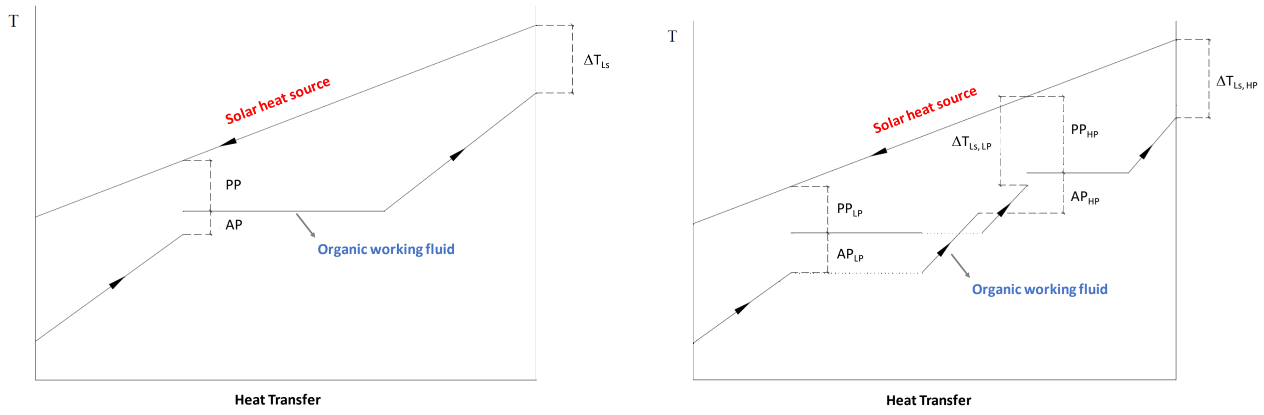

(**a**) (**b**)

Figure 8. Scheme and heat transfer-temperature diagram for two variants of evaporators: (**a**) Single-pressure with superheater; (**b**) Dual-pressure with low-pressure and high-pressure superheaters.

For the ORC layouts corresponding to Case 5 and Case 6, the extraction pressure is selected strategically between condensation and evaporation pressures with the aim to obtain the maximum thermodynamic efficiency of each cycle.

Table 2. Input data for ORC model

Parameter	**Value**
Condensation temperature – T_1	90 ºC
Turbine efficiency – η_{turb}	85%
Pump isentropic efficiency - $\eta_{ORC,pump}$, $\eta_{Evap,pump}$,	70%
Recuperator efficiency* – η_{REC}	70%
Superheating** – ΔT_{SH}	10 ºC
Live steam outlet temperature*** – T_{LS}	$T_{1'}$ - 25 ºC
Live steam outlet temperature ** – T_{LS}	$T_{1'}$ - 25ºC - ΔT_{SH}
Pinch Point – PP	8 K
Approach Point – AP	5 K

* For recuperated cycles (Case 3, 4, 5, 6)
** For superheated cycles (Case 2, 4, 5, 6)
*** For non-superheated cycles (Case 1, 3)

With regard to the absorption heat-pump, several modelling studies with experimental validation for specific and generic absorption machines can be found in the literature reviewed [22-25]. In the proposed absorption heat-pump model there is a total of 18 states each of which is determined by its temperature, pressure, enthalpy, flow, H_2O/LiBr concentration, etc. The assumptions used in the single-effect absorption chiller are:

- Saturated liquid solution at states 1 and 4;
- Subcooled liquid solution at states 2, 3 and 5;
- Vapor-liquid mixture solution at state 6;
- Superheated water vapor at state 7;
- Saturated water liquid at high pressure at state 8;
- Vapor-liquid mixture (water) at state 9;
- Saturated water vapor at low pressure at state 10;

The input data used in the Absorption Heat-Pump model is given in Table 3. The selected values are reasonable, and conservative to avoid the formation of crystals from the H_2O/LiBr solution.

Table 3. Input data for Absorption Heat-Pump model

Parameter	Value
Maximum solution concentration, – $x_{4''}$	65 %
Condensation temperature – $T_{13''}$; $T_{15''}$	20 ºC
Condensation mass flow rate	12 kg/s
Evaporation temperature – $T_{17''}$	12 ºC
Evaporation mass flow rate	15 kg/s
Solution heat exchanger efficiency – $\eta_{sol.he}$	70%
UA desorber	30 kW/K
UA condenser	70 kW/K
UA absorber	20 kW/K
UA evaporator	30 kW/K

3. Results and discussion

In the framework of the above constraints and assumptions, the methodology pursued to analyse the CCHP configuration variants from the thermodynamic viewpoint is organized as follow. First of all, for a given configuration and a given working fluid, an analysis of each pair is performed according to the nominal conditions indicated in Tables 1-3. Then, a systematic comparison of each combination is carried out by means of the evaluation of the performance indexes indicated in Section 2.1. Thereafter, a parametric approach is conducted for the best pair (configuration variant & working fluid) to evaluate the effects of different system operating parameters on the energy and exergy efficiency of the ORC and on the overall CCHP system performance. Finally, for each of the identified best pair, a muti-objective optimization study is performed based on the same operating parameters following the criteria of system energy and exergy.

With such methodology, it is possible to determine the best performing CCHP variant in terms of system energy and exergy efficiency within the six analysed alternatives and for the seven organic working fluids, and on the other hand, to assess how the variation of some design operating parameters can affect the performance of the system and what the optimum values for such parameters are for each variant in terms of system performance.

3.1. Analysis of CCHP variants

Tables 4-6 represent the energy and exergy efficiency of the ORC and on the overall CCHP system performance for each of the proposed CCHP configurations and organic working fluids at nominal conditions indicated in Tables 1-3.

Table 4. Results for Case 1: CCHP with single-pressure ORC Simple cycle (1P SC)

Fluid	$\eta_{en,ORC}$ [%]	$\eta_{ex,ORC}$ [%]	$\eta_{en,tri}$ [%]	$\eta_{ex,tri}$ [%]	W_{turb} [kW]	Q_e [kW]	Q_a [kW]	Q_c [kW]
Toluene	9.64	10.33	166.10	26.70	10.58	48.19	228.83	241.42
Benzene	**9.74**	**10.43**	**165.90**	**26.95**	**10.68**	**49.15**	**228.49**	**241.06**
n-heptane	8.51	9.12	167.80	23.65	9.37	42.98	232.97	245.83
n-octane	8.56	9.16	167.70	23.78	9.42	42.77	232.80	245.65
n-nonane	8.53	9.14	167.70	23.71	9.39	42.42	232.89	245.74
n-decane	8.53	9.13	167.70	23.70	9.39	42.27	232.91	245.76
MDM	7.32	7.84	169.50	20.44	8.10	36.51	237.32	250.46

Table 5. Results for Case 2: CCHP with single-pressure ORC superheated cycle (1P SH)

Fluid	$\eta_{en,ORC}$ **[%]**	$\eta_{ex,ORC}$ **[%]**	$\eta_{en,tri}$ **[%]**	$\eta_{ex,tri}$ **[%]**	W_{turb} **[kW]**	Q_e **[kW]**	Q_a **[kW]**	Q_c **[kW]**
Toluene	9.58	10.26	166.20	10.51	47.85	229.06	302.71	241.67
Benzene	**9.71**	**10.40**	**166.00**	**10.65**	**48.99**	**228.59**	**302.10**	**241.17**
n-heptane	8.36	8.95	168.00	9.21	42.19	233.52	308.45	246.42
n-octane	8.38	8.98	168.00	9.23	41.87	233.44	308.35	246.33
n-nonane	8.36	8.95	168.00	9.21	41.55	233.52	308.45	246.41
n-decane	8.35	8.94	168.00	9.20	41.39	233.56	308.50	246.45
MDM	7.10	7.60	169.80	7.86	35.41	238.12	314.38	251.31

Table 6. Results for Case 3: CCHP with single-pressure ORC recuperated cycle (1P REC)

Fluid	$\eta_{en,ORC}$ **[%]**	$\eta_{ex,ORC}$ **[%]**	$\eta_{en,tri}$ **[%]**	$\eta_{ex,tri}$ **[%]**	W_{turb} **[kW]**	Q_e **[kW]**	Q_a **[kW]**	Q_c **[kW]**
Toluene	**10.71**	**11.47**	**164.50**	**11.72**	53.50	224.94	297.41	237.29
Benzene	10.53	11.28	164.80	11.53	53.18	225.58	298.23	237.97
n-heptane	10.45	11.19	164.90	11.44	52.78	225.88	298.61	238.28
n-octane	10.57	11.32	164.70	11.57	52.83	225.44	298.05	237.82
n-nonane	10.63	11.39	164.60	11.63	52.84	225.22	297.77	237.59
n-decane	10.66	11.41	164.60	11.66	52.81	225.14	297.66	237.50
MDM	10.20	10.92	165.30	11.17	50.87	226.80	299.80	239.27

Table 7. Results for Case 4: CCHP with single-pressure ORC recuperated superheated cycle (1P REC+SH)

Fluid	$\eta_{en,ORC}$ **[%]**	$\eta_{ex,ORC}$ **[%]**	$\eta_{en,tri}$ **[%]**	$\eta_{ex,tri}$ **[%]**	W_{turb} **[kW]**	Q_e **[kW]**	Q_a **[kW]**	Q_c **[kW]**
Toluene	**10.95**	**11.73**	**164.20**	**11.97**	**54.69**	**224.06**	**296.27**	**236.35**
Benzene	10.83	11.60	164.30	11.84	54.63	224.50	296.84	236.82
n-heptane	10.67	11.42	164.60	11.67	53.82	225.10	297.61	237.45
n-octane	10.76	11.52	164.40	11.76	53.73	224.77	297.18	237.10
n-nonane	10.78	11.55	164.40	11.79	53.57	224.68	297.07	237.01
n-decane	10.79	11.55	164.40	11.80	53.47	224.65	297.03	236.97
MDM	10.29	11.02	165.10	11.27	51.32	226.46	299.36	238.91

Table 8. Results for Case 5: CCHP with single-pressure ORC regenerative recuperated superheated cycle (1P REG+REC+SH)

Fluid	$\eta_{en,ORC}$ **[%]**	$\eta_{ex,ORC}$ **[%]**	$\eta_{en,tri}$ **[%]**	$\eta_{ex,tri}$ **[%]**	W_{turb} **[kW]**	Q_e **[kW]**	Q_a **[kW]**	Q_c **[kW]**
Toluene	**11.24**	**12.04**	**163.70**	**12.29**	**56.19**	**222.98**	**294.89**	**235.21**
Benzene	11.17	11.96	163.80	12.20	56.41	223.26	295.24	235.50
n-heptane	10.77	11.53	164.40	11.78	54.42	224.71	297.11	237.04
n-octane	10.90	11.68	164.20	11.92	54.51	224.22	296.48	236.53
n-nonane	10.96	10.55	164.10	11.98	54.49	224.02	296.22	236.31
n-decane	10.99	11.77	164.10	12.02	54.49	223.91	296.08	236.19
MDM	10.36	11.09	165.00	11.34	51.67	226.23	299.07	238.66

Table 9. Results for Case 6: CCHP with dual-pressure ORC recuperated superheated cycle (2P REC+SH).

Fluid	$\eta_{en,ORC}$ **[%]**	$\eta_{ex,ORC}$ **[%]**	$\eta_{en,tri}$ **[%]**	$\eta_{ex,tri}$ **[%]**	W_{turb} **[kW]**	Q_e **[kW]**	Q_a **[kW]**	Q_c **[kW]**
Toluene	**10.31**	**11.04**	**165.10**	**11.29**	**51.46**	**226.40**	**299.29**	**238.84**
Benzene	10.18	10.90	165.30	11.15	51.30	226.89	299.91	239.36
n-heptane	10.10	10.82	165.40	11.07	50.96	227.15	300.25	239.64
n-octane	10.09	10.81	165.40	11.06	50.39	227.20	300.31	239.69
n-nonane	10.10	10.82	165.40	11.07	50.19	227.16	300.26	239.65
n-decane	10.11	10.83	165.40	11.08	50.11	227.12	300.21	239.61
MDM	9.67	10.36	166.00	10.61	48.21	228.72	302.28	241.31

The performance indexes indicated in Tables 4-9 show that for the six CCHP configurations and the seven organic working fluids analysed, the best performing variant is the CCHP with single-pressure ORC regenerative recuperated superheated cycle (Case 5) with toluene as a working fluid. The achieved energy and exergy efficiency are: 11.24% and 12.04% respectively for the ORC, and 163.7% and 12.3% respectively for the CCHP. The electricity, cooling and heating productions are 56.2 kW, 222.3 kW and 530.1 kW respectively. On average for the seven working fluids considered, in terms of ORC energy efficiency the Case 5 is 25% more efficient than Case 1 (1P SC). In terms of which organic working fluid is best suited depending on the configuration, benzene performs best for Cases 1-2, and toluene for Cases 3-6.

A CCHP with single-pressure ORC superheated cycle (Case 2) only results in an increase in efficiency if a recovery stage is available downstream of the turbine. The performance indexes show that on average for the seven working fluids considered, in terms of ORC energy efficiency the Case 2 is 1.6% less efficient than Case 1 (1P SC).

The main objective in evaporator design is to minimise losses and maximise heat recovery from the solar heat source. This is achieved by introducing multiple pressure levels, as the temperature curves of the heat source and the organic fluid are better adapted each other (see Figure 8 (b)), increasing the efficiency of the evaporator, but also its complexity and cost, as more heat exchangers are introduced. The results obtained for the Case 6 (2P REC+SH) show that the fact to include two pressure levels in the evaporator does not imply a performance improvement of the CCHP system in comparison with Case 3 (1P REC), Case 4 (1P REC+SH) and Case 5 (1P REG+REC+SH); in fact, on average for the seven working fluids considered, in terms of ORC energy efficiency the Case 6 is about 8% less efficient than Case 5. This is explained because the temperature of the heat source at the evaporator outlet is constrained by the close loop of SPTCs, what impact on the capacity of the dual-pressure evaporator to maximise the heat recovery from the solar heat source.

3.2. *Parametric analysis*

In this subsection a parametric approach is conducted for the best pair analysed previously (configuration variant & working fluid) to evaluate the effects of different system parameters on the energy and exergy efficiency of the ORC and on the overall CCHP system performance.

3.2.1. Effect of the solar field outlet temperature

The selection of an optimal evaporation temperature for the ORC is determined by the heat delivered by the solar field. This study aims to illustrate the influence of the solar field outlet temperature, varying in the range of 180 – 260 ºC, on the efficiency of the ORC and on the overall trigeneration system. Table 10 and Figure 9 represent the system performance and electrical and thermal generation for each analysed pair.

Table 10. Results of the parametric simulation with the solar field outlet temperature ($T_{1'}$)

Pair	$T_{1'}$ [ºC]	$\eta_{en,ORC}$ [%]	$\eta_{ex,ORC}$ [%]	$\eta_{en,tri}$ [%]	$\eta_{ex,tri}$ [%]	W_{turb} [kW]	Q_e [kW]	Q_a [kW]	Q_c [kW]	COP_{cool}	COP_{heat}
Case 1. w/ Benzene	180	8.14	8.72	168.70	8.98	40.92	234.87	310.19	247.85	0.7268	1.727
	190	8.98	9.62	167.30	9.87	45.23	231.54	305.91	244.31	0.7266	1.727
	200	9.74	10.43	165.90	10.68	49.15	228.49	301.98	241.06	0.7264	1.726
	220	11.04	11.82	163.60	12.06	56.00	223.08	295.01	235.31	0.7261	1.726
	240	12.08	12.94	161.50	13.18	61.70	218.41	289.06	230.34	0.7256	1.726
	260	12.92	13.83	159.60	14.07	66.43	214.41	283.92	226.09	0.7253	1.725
Case 2. w/ Benzene	180	8.12	8.69	168.70	8.95	40.77	234.96	310.30	247.94	0.7268	1.727
	190	8.96	9.59	167.30	9.84	45.07	231.64	306.03	244.41	0.7266	1.727
	200	9.71	10.40	166.00	10.65	48.99	228.59	302.10	241.17	0.7264	1.726
	220	11.01	11.79	163.60	12.04	55.83	223.17	295.12	235.40	0.7261	1.726
	240	12.07	12.92	161.50	13.16	61.54	218.47	289.14	230.41	0.7256	1.726
	260	12.91	13.83	159.60	14.06	66.32	214.42	283.93	226.10	0.7253	1.725
Case 3. w/ Toluene	180	8.75	9.37	167.80	9.63	43.6	232.65	307.33	245.49	0.7266	1.727
	190	9.76	10.45	166.10	10.71	48.71	228.69	302.23	241.27	0.7264	1.726
	200	10.71	11.47	164.50	11.72	53.50	224.94	297.41	237.29	0.7262	1.726
	220	12.42	13.30	161.50	13.53	62.21	217.99	288.52	229.90	0.7256	1.726
	240	13.90	14.88	158.80	15.12	69.89	211.76	280.52	223.28	0.7251	1.725
	260	15.16	16.23	156.30	16.46	76.56	206.19	273.36	217.36	0.7247	1.725
Case 4. w/ Toluene	180	8.96	9.59	167.50	9.85	44.61	231.90	306.36	244.69	0.7266	1.727
	190	9.99	10.70	165.80	10.95	49.81	227.86	301.17	240.40	0.7264	1.726
	200	10.95	11.73	164.20	11.97	54.69	224.06	296.27	236.35	0.7261	1.726
	220	12.69	13.59	161.10	13.82	63.55	217.00	287.24	228.84	0.7255	1.726
	240	14.20	15.20	158.30	15.43	71.36	210.67	279.11	222.11	0.725	1.725
	260	15.44	16.57	155.90	16.80	77.90	205.21	272.11	216.32	0.7246	1.725
Case 5. w/ Toluene	180	9.02	9.66	167.40	9.92	44.96	231.65	306.05	244.43	0.7266	1.727
	190	10.18	10.90	165.50	11.15	50.78	227.18	300.28	239.67	0.7263	1.726
	200	11.24	12.04	163.70	12.29	56.19	222.98	294.89	235.21	0.7261	1.726
	220	13.16	14.09	160.40	14.33	66.01	215.26	285.01	226.99	0.7254	1.725
	240	14.83	15.87	157.40	16.10	74.71	208.36	276.15	219.66	0.7249	1.725
	260	16.27	17.42	154.60	17.64	82.45	202.12	268.15	213.04	0.7243	1.724
Case 6. w/ Toluene	180	8.15	8.73	168.70	8.98	40.57	234.84	310.15	234.84	0.7268	1.727
	190	9.27	9.93	166.80	10.18	46.22	230.48	304.54	230.48	0.7265	1.727
	200	10.31	11.04	165.10	11.29	51.46	226.40	299.29	226.40	0.7263	1.726
	220	12.23	13.10	161.80	13.33	61.24	218.67	289.34	218.67	0.7256	1.726
	240	13.93	14.91	158.70	15.14	70.02	211.65	280.38	211.65	0.7251	1.725
	260	15.45	16.54	155.80	16.77	78.07	205.11	271.98	205.11	0.7246	1.725

As can be observed in Table 9 and Figure 10, higher values of the solar field outlet temperature mean an increase in ORC energy and exergy efficiency, and CCHP exergy efficiency. This is due to a higher temperature of the heat source causes a higher organic fluid evaporation pressure in the ORC leading to higher heat recovery efficiency in the evaporator. For Case 5, which is the best performing variant, with the increase of the heat source inlet temperature, the efficiency of the ORC increases from 9.0% to 16.3%. In terms of relative increase for the electricity produced by the turbine, the increase of the heat source inlet temperature of 180–260 °C represents an increase of 83% (from 45.0 kW to 82.5 kW).

For the CCHP with dual-pressure ORC (Case 6), the relative increase either for the ORC energy efficiency and electricity produce by the turbine with respect the increase of the heat source inlet temperature of 180–260 °C is significantly greater: 90% for the ORC efficiency (from 8.2% to 15.5%) and 92% for electricity produce by the turbine (from 41.6 kW to 78.1 kW).

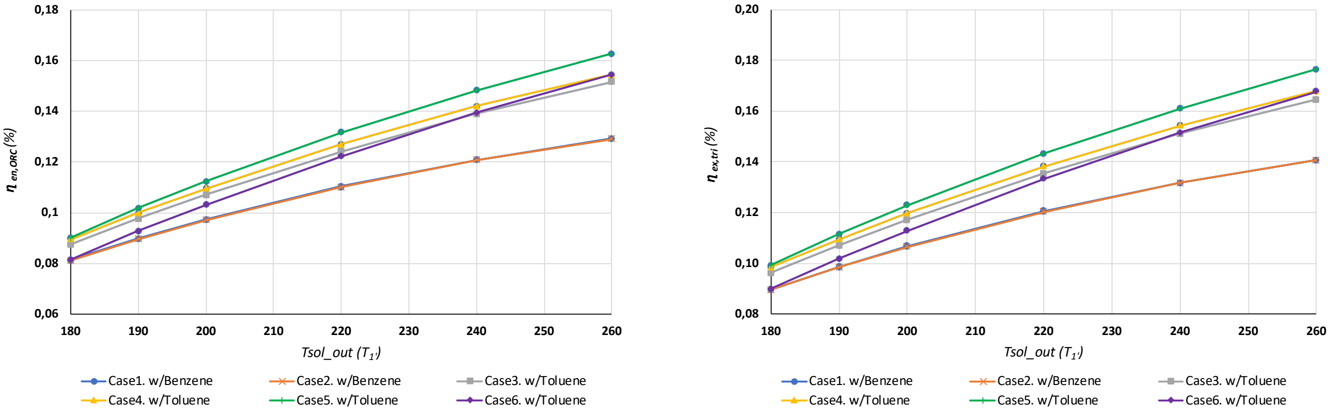

(**a**) (**b**)

Figure 9. Effect of the solar field outlet temperature on: (**a**) ORC energy efficiency; (**b**) CCHP exergy efficiency

3.2.2. Effect of ORC condensation temperature

The single-effect absorption heat-pump requires a certain heat input in the desorber within a specific temperature range for its operation. This inlet temperature is determined by the condensation temperature of the ORC, so it is important to identify which is the optimal operating temperature based on the production that needs to be prioritized.

In this study, the effect of the ORC condensation temperature is examined from 85 to 105 ºC, and system performance and electrical and thermal generation for each analysed pair are presented in Table 11 and Figures 10.

Table 11. Results of the parametric simulation with ORC condensation temperature (T_1)

Pair	T_1 [ºC]	$\eta_{en,ORC}$ [%]	$\eta_{ex,ORC}$ [%]	$\eta_{en,tri}$ [%]	$\eta_{ex,tri}$ [%]	W_{turb} [kW]	Q_e [kW]	Q_a [kW]	Q_c [kW]	COP_{cool}	COP_{heat}
Case 1. w/ Benzene	85	10.26	10.99	165.20	11.24	51.75	226.57	299.50	239.02	0.7263	1.726
	90	9.74	10.43	165.90	10.68	49.15	228.49	301.98	241.06	0.7264	1.726
	95	9.21	9.87	166.70	10.12	46.55	230.42	304.45	243.11	0.7265	1.727
	100	8.68	9.30	167.50	9.55	43.94	232.34	306.94	245.16	0.7266	1.727
	105	8.15	8.73	168.30	8.99	41.32	234.28	309.43	247.23	0.7267	1.727
Case 2. w/ Benzene	85	10.24	10.97	165.20	11.22	51.60	226.65	299.61	239.11	0.7263	1.726
	90	9.71	10.40	166.00	10.65	48.99	228.59	302.10	241.17	0.7264	1.726
	95	9.18	9.83	166.80	10.08	46.37	230.52	304.59	243.23	0.7265	1.727
	100	8.65	9.26	167.60	9.52	43.74	232.46	307.09	245.29	0.7266	1.727
	105	8.12	8.69	168.30	8.95	41.11	234.41	309.60	247.36	0.7267	1.727
Case 3. w/ Toluene	85	11.31	12.11	163.60	12.35	56.45	222.71	294.59	234.92	0.7259	1.726
	90	10.71	11.47	164.50	11.72	53.50	224.94	297.41	237.29	0.7262	1.726
	95	10.11	10.82	165.40	11.07	50.53	227.14	300.23	239.62	0.7263	1.726
	100	9.51	10.18	166.30	10.43	47.55	229.34	303.07	241.97	0.7265	1.726
	105	8.90	9.53	167.20	9.79	44.56	231.55	305.92	244.32	0.7266	1.727
Case 4. w/ Toluene	85	11.56	12.38	163.20	12.62	57.70	221.78	293.40	233.93	0.7259	1.726
	90	10.95	11.73	164.20	11.97	54.69	224.06	296.27	236.35	0.7261	1.726
	95	10.34	11.07	165.10	11.32	51.66	226.30	299.15	238.73	0.7263	1.726
	100	9.72	10.41	166.00	10.66	48.62	228.54	302.04	241.12	0.7264	1.726
	105	9.11	9.75	166.90	10.00	45.57	230.80	304.95	243.52	0.7265	1.727
Case 5.	85	11.92	12.77	162.70	13.01	59.55	220.46	291.69	232.52	0.7258	1.726

w/ Toluene	90	11.24	12.04	163.70	12.29	56.19	222.98	294.89	235.21	0.7261	1.726
	95	10.55	11.30	164.70	11.55	52.77	225.51	298.14	237.89	0.7262	1.726
	100	9.85	10.55	165.80	10.80	49.28	228.09	301.45	240.63	0.7264	1.726
	105	9.13	9.77	166.90	10.03	45.70	230.72	304.85	243.44	0.7265	1.727
Case 6. w/ Toluene	85	10.96	11.73	164.10	11.98	54.65	224.04	296.24	236.33	0.7261	1.726
	90	10.31	11.04	165.10	11.29	51.46	226.40	299.29	238.84	0.7263	1.726
	95	9.66	10.34	166.10	10.59	48.24	228.78	302.35	241.37	0.7264	1.726
	100	9.00	9.64	167.00	9.90	45.00	231.17	305.43	243.92	0.7266	1.727
	105	8.35	8.94	168.00	9.20	41.74	233.57	308.52	246.47	0.7267	1.727

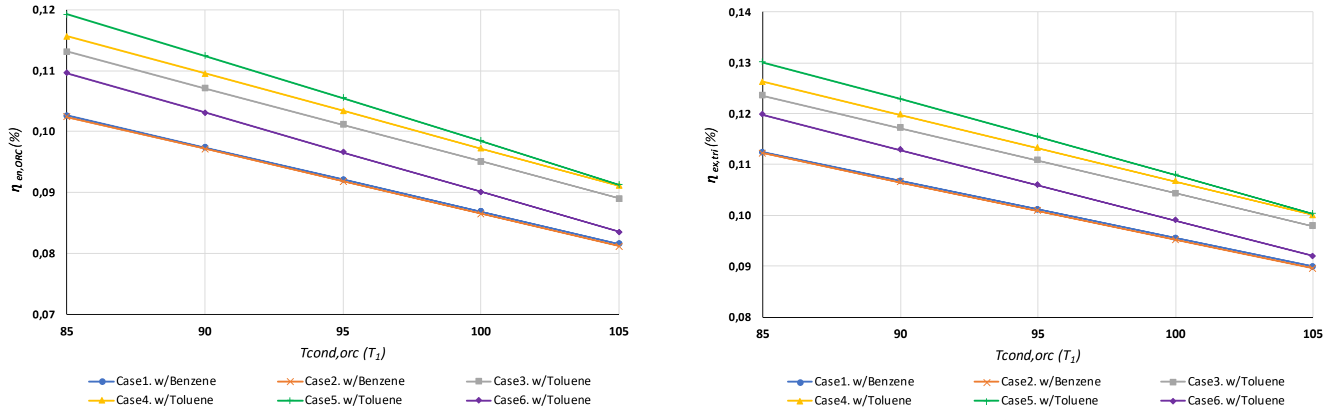

Figure 10. Effect of ORC condensation temperature on: (**a**) ORC energy efficiency; (**b**) CCHP exergy efficiency

ORC condensation temperature can be a good parameter for controlling the cooling and heating power to be produced by the absorption heat-pump. It is observed that as the ORC condensation temperature increases, both the ORC energy efficiency and CCHP exergy efficiency decrease; the lower the condensing pressure the higher the capacity to extract work from the turbine. For Case 5, with the increase of the ORC condensation temperature, the efficiency of the ORC decreases from 9.1% to 11.9%; in relative terms for the electricity produced by the turbine, the increase of the ORC condensation temperature of 85–105 °C represents a decrease of 23% (from 59.6 kW to 45.7 kW).

Regarding the energy efficiency of the trigeneration system, the effect is the opposite, as the condensation temperature increases the overall efficiency of the system also increases because the heat input to the absorption heat-pump desorber is greater and therefore the heat of the evaporator, absorber and condenser are also greater.

3.3. *Optimization analysis*

The optimization procedure proposed is based on the optimization of the analysed operating parameters (see Table 12), and not of the system devices, following strictly energy and exergy efficiency criteria. Therefore, a multi-objective optimization approach is considered for each of the identified best pair requiring the simultaneous satisfaction of certain objectives, that is the ORC energy efficiency (Equation (1)) and CCHP exergy efficiency (Equation (7)).

Table 12. Optimization variables

Parameter	Default value	Examined range
Solar field outlet temperature – $T_{1'}$	200 ºC	[180 - 260] ºC
ORC Condensation temperature – T_1	90 ºC	[85 - 105] ºC

The Pareto front is probably one of the most common approaches used for multi-objective optimization problems in thermodynamics [26-27]. However, the most straightforward approach to solve these problems is the weighted sum method [28-29], that combines all the multi-objective functions into one scalar by summing the corresponding objectives with some appropriate weights. For the trigeneration system analysis considered in this paper, the bi-objective optimization is constructed by summing the two before mentioned objectives with some appropriate weights, as follows:

$$MAX\ (MOF = w_1 \cdot \eta_{en,ORC} + w_2 \cdot \eta_{ex,tri}) \\ 0 \le w_1, w_2 \le 1 \\ w_1 + w_2 = 1 \tag{17}$$

where, w_1 and w_2 are the weighting coefficients for the ORC energy efficiency and CCHP exergy efficiency, respectively. Though any set of optimal solutions can be chosen by selecting the desired values of weighting coefficients, the two objectives are assumed to be of the same importance. The "Conjugate Directions Method" which is supported by EES is used in the bi-objective optimal design (Equation 17). The results obtained for each of the identified best pair are shown in Table 13.

Table 13. Results of the multi-objective optimization

Pair	Opt. Variables		Objectives		Performance indexes							
	$T_{1'}$ [ºC]	T_1 [ºC]	$\eta_{en,ORC}$ [%]	$\eta_{ex,tri}$ [%]	$\eta_{ex,ORC}$ [%]	$\eta_{en,tri}$ [%]	W_{turb} [kW]	Q_e [kW]	Q_a [kW]	Q_c [kW]	COP_{cool}	COP_{heat}
Case 1. w/ Benzene	260	85	13.33	14.53	14.30	158.90	68.56	218.80	281.85	224.38	0.7252	1.725
Case 2. w/ Benzene	260	85	13.36	14.54	14.30	158.90	68.47	212.79	281.84	224.74	0.7252	1.725
Case 3. w/ Toluene	260	85	15.67	17.01	16.78	155.50	79.08	204.30	270.94	215.35	0.7245	1.725
Case 4. w/ Toluene	260	85	16.02	17.38	17.16	155.00	80.78	203.02	269.30	213.99	0.7244	1.724
Case 5. w/ Toluene	260	85	16.82	18.23	18.02	153.80	85.20	200.07	265.51	210.86	0.7241	1.724
Case 6. w/ Toluene	260	85	16.00	17.36	17.14	155.00	80.78	203.10	269.39	214.07	0.7244	1.724

The obtained results remark that the optimum design for all the analysed cases is produced for the maximum solar field outlet temperature (260 ºC) and the minimum ORC condensation temperature (85ºC). The best performing pair is Case 5 with toluene, presenting values of ORC energy efficiency and CCHP exergy efficiency of 16.82% and 18.23%, respectively. In comparison with nominal design conditions, the optimum design is in terms of ORC energy efficiency 50% more efficient.

4. Conclusions

A comprehensive and systematic comparative thermodynamic analysis of six different solar-heated CCHP systems based on ORC and absorption heat-pump is conducted. Any configuration can produce electricity, heating and cooling in temperature levels ideal for building or small-medium industry applications. The most suitable CCHP configuration has been identified in terms of system energy and exergy efficiency, as well as the best working fluid for each configuration variant. Through parametric and muti-objective optimization analysis it has been possible to determine how the solar field outlet temperature and the ORC condensation temperature affect the performance of the CCHP system for each best pair (configuration variant & working fluid). The main findings of the study are summarized below:

- For the six CCHP configurations and the seven organic working fluids analysed, the best performing variant is the CCHP with single-pressure ORC regenerative recuperated superheated cycle (Case 5) with toluene as a working fluid. The achieved energy and exergy efficiency are: 11.24% and 12.04% respectively for the ORC, and 163.7% and 12.3% respectively for the CCHP. The electricity, cooling and heating productions are 56.2 kW, 222.3 kW and 530.1 kW respectively.
- For the seven organic working fluids analysed, benzene performs best for Cases 1-2, and toluene for Cases 3-6.
- At nominal conditions and on average for the seven working fluids considered, the Case 5 is about 25% more efficient than Case 1, and about 8% more efficient than Case 6 in terms of ORC energy efficiency.
- A CCHP with single-pressure ORC superheated cycle (Case 2) only results in an increase in efficiency if a recovery stage is available downstream of the turbine.
- The use of a dual-pressure evaporator does not imply a performance improvement of the CCHP system if the temperature of the heat source at the evaporator outlet is constraint.
- A higher temperature of the solar heat source causes a higher organic fluid evaporation pressure in the ORC leading to higher heat recovery efficiency in the evaporator and in CCHP efficiency. For Case 5 with toluene, the electricity produced by the turbine presents an increase of 83% as the increase of the heat source inlet temperature from 180 to 260 °C.
- As the ORC condensation temperature increases, both the ORC energy efficiency and CCHP exergy efficiency decrease. For Case 5 with toluene, the increase of the ORC condensation temperature from 85 to 105 °C represents a decrease of 23% of the electricity produced by the turbine.
- The optimum design conditions for all the analysed cases are produced for the maximum solar field outlet temperature (260 ºC) and the minimum ORC condensation temperature (85ºC). For Case 5 with toluene, in comparison with nominal design conditions, the optimum design is 50% more efficient in terms of ORC energy efficiency.

Nomenclature

Symbols

h	*heat transfer coefficient, W/(m² K)*
$\dot{m}$	*mass flow rate, kg/s*
T	*temperature, °C*
ΔT	*temperature difference, °C*
η	*efficiency*
W	*electric power, kW*
Q	*thermal power, kW*
$\dot{q}'$	*heat rate per SPTC unit length, kW/m*
w_{ap}	*aperture width of SPTC, m*
L	*length of SPTC, m*
N	*number of SPTCs*
θ	*solar incidence angle on the SPTC, º*

Acronyms

CCHP	*combined cooling heating and power*
ORC	*organic Rankine cycle*
SPTC	*solar parabolic trough collector*

Subscripts

en	*energy*
ex	*exergy*
sol	*solar field*
0	*atmospheric conditions*
in	*inlet*
out	*inlet*
turb	*turbine*
cond	*heat conduction*
conv	*heat convection*
rad	*heat radiation*
SolAbs	*solar absorption*
tri	*trigeneration*
d	*heat-pump desorber*
a	*heat-pump absorber*
s.he	*heat-pump solution heat exchanger*
c	*heat-pump condenser*

REC	*recuperator heat exchanger or recuperated cycle*	*e*	*heat-pump evaporator*
REG	*regenerative cycle*	*Evap.pump*	*evaporator pump*
SC	*simple cycle*	*s.pump*	*solution pump*
SH	*superheater heat exchanger or superheated cycle*	*cool*	*heat-pump cooling mode*
DNI	*direct normal irradiance*	*heat*	*heat-pump heating mode*
LS	*live steam*		
PP	*pinch point*		
AP	*approach point*		
COP	*coefficient of performance*		
UA	*overall heat transfer coefficient*		

References

1. Al-Sulaiman F.A., Hamdullahpur F., Dincer I., "Trigeneration: a comprehensive review based on prime movers", International Journal of Energy Research, 2011, 35(3), p.233-258
2. Vélez F., Segovia J.J., Martín M.C., Antolín G., Chejnec F., Quijano A., "A technical, economical and market review of organic Rankine cycles for the conversion of low-grade heat for power generation", Energy Conversion and Management 69, 2013, p.209-216
3. Quoilin S., Van Den Broek M., Declaye S., Dewallef P., Lemort V., "Techno-economic survey of Organic Rankine Cycle (ORC) systems", Renewable and Sustainable Energy Reviews 22, 2013, p.168-186
4. Villarini M., Bocci E., Moneti M., Di Carlo A., Micangeli A., "State of art of small scale solar powered ORC systems: a review of the different typologies and technology perspectives", Energy Procedia 45, 2014, p.257-267
5. Li J., Ge Z., Duan Y., Yang Z., Liu Q., "Parametric optimization and thermodynamic performance comparison of single-pressure and dual-pressure evaporation organic Rankine cycles", Applied Energy 217, 2018, p.409-421
6. Fernández-Guillamón A.; Molina-García Á.; Vera-García F.; Almendros-Ibáñez J.A., "Organic Rankine Cycle Optimization Performance Analysis Based on Super-Heater Pressure: Comparison of Working Fluids", Energies 2021, 14, 2548
7. Manente G., Lazzaretto A., Bonamico E., "Design guidelines for the choice between single and dual pressure layouts in organic Rankine cycle (ORC) systems", Energy 123, 2017, p.413-431
8. Branchini L., De Pascale A., Peretto A., "Systematic comparison of ORC configurations by means of comprehensive performance indexes", Applied Thermal Engineering 61, 2013, p.129-140
9. Delgado-Torres A.M., García-Rodríguez L., "Analysis and optimization of the low-temperature solar organic Rankine cycle (ORC)", Energy Conversion and Management 51, 2010, p.2846-2856
10. Villarini M., Bocci E., Di Carlo A., Sbordone D., "Technical-Economic Analysis of an Innovative Small Scale Solar Thermal - ORC Cogenerative System", ICCSA 2013, Part II, LNCS 7972, p.271-287
11. Hassoun A., Dincer I., "Analysis and performance assessment of a multigenerational system powered by Organic Rankine Cycle for a net zero energy house", Applied Thermal Engineering 76, 2015, p.25-36
12. Khalid F., Dincer I., Rosen M.A., "Thermoeconomic analysis of a solar-biomass integrated multigeneration system for a community", Applied Thermal Engineering 120, 2017; p.645-653
13. Bellos E., Tzivanidis C., "Multi-objective optimization of a solar driven trigeneration system", Energy 149, 2018, p.47-62
14. Tauseef Nasir M., Ekwonu M.C.; Park Y.; Abolfazli Esfahani J.; Kim, K.C., "Assessment of a District Trigeneration Biomass Powered Double Organic Rankine Cycle as Primed Mover and Supported Cooling", Energies 2021, 14, 1030
15. García-Domínguez J., Blanco-Marigorta A. M., Marcos J. D., "Thermodynamic analysis and optimization of a combined cooling, heating, and power system using Organic Rankine Cycles (ORC) and solar parabolic trough collectors", 2020, 33rd International Conference on Efficiency, Cost, Optimization, Simulation and Environmental Impact of Energy Systems

16. Al-Sulaiman F.A., Hamdullahpur F., Dincer I., "Performance comparison of three trigeneration systems using organic rankine cycles", Energy 36, 2011, p.5741-5754
17. Al-Sulaiman F.A., Hamdullahpur F., Dincer I., "Performance assessment of a novel system using parabolic trough solar collectors for combined cooling, heating, and power production", Renewable Energy 48, 2012, p.161-172
18. Suleman F., Dincer I., Agelin-Chaab M., "Development of an integrated renewable energy system for multigeneration". Energy 78, 2014, p.196-204.
19. Bellos E., Tzivanidis C., "Parametric analysis and optimization of a solar driven trigeneration system based on ORC and absorption heat pump", Journal of Cleaner Production, 16110, 2017, p.493-509
20. Petela R., "Exergy of undiluted thermal radiation", Sol Energy 74(6), 2013, p.469-488
21. Forristall R., "Heat Transfer Analysis and Modeling of a Parabolic Trough Solar Receiver Implemented in Engineering Equation Solver", 2003, NREL/TP-550-34169, National Renewable Energy Laboratory
22. Liao X., Garland P., Radermacher R., "The modeling of air-cooled absorption chiller integration in CHP system", ASME International Mechanical Engineering Congress and Exposition IMECE2004-60308, 2004
23. Bakhtiari B., Fradette L., Legros R., Paris J., "A model for analysis and design of H_2O–LiBr absorption heat pumps", Energy Conversion and Management 52, 2011, p.1439-1448
24. Marcos J.D., Izquierdo M., Palacios E., "New method for COP optimization in water-and air-cooled single and double effect LiBr–water absorption machines", International journal of refrigeration 34 (6), 2011, p.1348-1359
25. Evola G., Le Pierre`s N., Boudehenn F., Papillon P., "Proposal and validation of a model for the dynamic simulation of a solar-assisted single-stage LiBr/water absorption chiller", International Journal of Refrigeration 36, 2013, p.1015-1028
26. Spelling J., Favrat D., Martin A., Augsburger G., "Thermoeconomic optimization of a combined-cycle solar tower power plant", Energy 41, 2012, p.113-120.
27. Baghernejad A., Yaghoubi M., Jafarpur K., "Exergoeconomic optimization and environmental analysis of a novel solar-trigeneration system for heating, cooling and power production purpose", Solar Energy 134, 2016, p.165-179
28. Kim I.Y., de Weck O.L., "Adaptive weighted-sum method for bi-objective optimization: Pareto front generation", Structural and Multidisciplinary Optimization, 2005, 29, p.149-158
29. Zare V., Mahmoudi S.M.S., Yari M., Amidpour M., "Thermoeconomic analysis and optimization of an ammonia-water power/cooling cogeneration cycle", Energy 47, 2012, p.271-283